Reports

Deep-Sea Erosion and Manganese Nodule Development in the Southeast Indian Ocean

Abstract. *Features exhibited by a large number of sea floor photographs together with the dating of 187 sediment cores from the southeast Indian Ocean have revealed extensive manganese nodule development and sediment erosion in deep basinal areas. The most extensive nodule field, with an area of* 10^6 *square kilometers, occurs in the northwestern sector of the South Australian Basin and is named the Southeast Indian Ocean Manganese Pavement. The crests and flanks of the adjacent mid-ocean ridge are, in contrast, free of nodules and marked by much less dynamic bottom water conditions.*

One of the major environmental requirements for the extensive development of deep-sea manganese nodules is a low or negative sedimentation rate, which allows accretion of nodules to continue uninterrupted by the accumulation of other particles. Many areas of the deep ocean floor have experienced, or are presently experiencing, long-term high-velocity bottom currents, which lead to the creation of disconformities over large areas (*1–3*). A clear relation between active erosion by bottom currents and the development of manganese nodule fields has been demonstrated, however, in only a few regions. The best example is the belt of manganese nodules underlying the Antarctic Circumpolar Current (*2, 4, 5*), which is the world's most active current system. Within this belt, manganese nodules may become sufficiently abundant to form a pavement with little intervening sediment; this is the case in the South Tasman Sea (*2*), where a very clear association with deep-sea current erosion has been demonstrated (*1, 2*). We report here the discovery of another extensive area of manganese nodules in the southeast Indian Ocean and show its relation to long-term deep-sea erosion by bottom currents.

We have determined the paleomagnetic and micropaleontological ages of 187 deep-sea sedimentary cores collected during six cruises of the U.S.N.S. *Eltanin* throughout the southeast Indian Ocean (*6*) between 70°E and 120°E and between Antarctica and 30°S. Our second series of relevant observations have been obtained from approximately 2800 deep-sea bottom photographs from 143 camera stations of *Eltanin*. The study area and sites of observations are shown in Fig. 1. A full account, including ages of cores, limits on the resolution of ages and the disconformity detection method, and the nature of bottom conditions, is presented elsewhere (*6*). Similar analyses were made previously in the Southern Ocean south of Australia and New Zealand (*2*) and in the South Pacific area (*7*), where paleomagnetically defined sedimentation rates were used to determine regional sedimentary patterns, so that long-term oceanographic controls of sediment distribution could be inferred.

A total of 42 of the cores examined contain disconformities separating sediments of various ages. As shown in Fig. 1, these cores largely occur in three regions: the Kerguelen Plateau, the northern sector of the South Indian Basin, and the western sector of the South Australian Basin. Of the 42 cores containing disconformities, 24 have a veneer of Recent to late Quaternary sediment. This sediment probably represents a relatively recent temporary waning of bottom water activity, but in some cases is a residual coarse fraction. Nine cores lack even a thin veneer of Recent to late Quaternary sediments, which indicates that in certain areas strong erosion has continued to the present day. Six of these cores occur in the vicinity of the Kerguelen Plateau, suggesting that very strong currents have probably persisted over the Kerguelen Plateau, in contrast to the erosional pulses of adjacent deep basins. Undisturbed sequences occur throughout most of the mid-ocean ridge system separating these two major basins.

Qualitative features in bottom photographs have been successfully used to enhance the mapping of current velocities (*2, 5, 8*). The presence of manganese nodules, ripple marks, scour, and distinct current-formed lineations constitutes evidence for strong current activity. Smooth sediment surfaces and the presence of abundant to common bioturbation are evidence of moderate to weak currents. Areas with abundant bioturbation or smooth sediment surfaces (or quiet bottom conditions) occur throughout almost all of the mid-ocean ridge system and on Broken Ridge (Fig. 1). These bottom features also occur in less extensive areas in the southeastern sector of the South Indian Basin and close to Antarctica. In sharp contrast, areas of sea floor that typically display features resulting from strong bottom currents occur extensively throughout the northwestern sector of the South Indian Basin and the South Australian Basin. These features also occur on the flanks and crest of the Kerguelen Plateau. Thus, the areas displaying highly active bottom currents at the present sediment surface are those which contain most of the cores with disconformities involving much older sediments.

The bottom photographs reveal previously undetected vast concentrations of manganese nodules in the northwestern sector of the South Australian Basin immediately south of Broken Ridge and Naturaliste Plateau (Fig. 1). A large part of this region is characteristically covered by dense packings of manganese nodules that form a manganese pavement. We name this feature the Southeast Indian Ocean Manganese Pavement. The manganese nodules making up much of this surface appear to be spherical, although in some areas botryoidal nodules occur. If the distribution is continuous between the areas in the bottom photographs that display these features (see Fig. 1), the concentrated nodules may cover an area as large as 10^6 km^2. The proximity of this pavement to the Perth-Fremantle industrial area of Western Australia makes it of some prospective economic interest. We believe that this pavement, like that of the South Tasman Sea (*1, 2, 9*), has accumulated in association with prolonged, high-velocity bottom currents. Other occurrences of abundant manganese nodules in the southeast Indian Ocean are more scattered, being mostly in the northwestern sector of the South Indian Basin. These do not appear to form large pavements.

The availability of both bottom photographs and cores makes it possible to determine the long-term principal paths (if not the directions) of bottom water circulation through the region. Directions along the paths can be inferred from hydrographic requirements of the circum-Antarctic current system. It is clear from Fig. 1 that major bottom current activity occurs over much of the crest and flanks of the Kerguelen Plateau to depths of at least 1700 m. The presence of several cores containing disconformities, some of which reach Eocene to Cretaceous age, is strong evidence for continued major bottom water erosion over the Kerguelen Plateau. While sediment of this age at or near the sediment-water interface could result from tectonic activity, seismic profiles taken over the Kerguelen Plateau confirm that major sediment erosion has occurred (*10*). Furthermore, bottom photographs from the crest and flanks of the Kerguelen Plateau invariably display features created by strong to very strong currents, even at the relatively shallow depths involved. The Kerguelen Plateau forms a major north-south trending barrier to the meridional flow of deep Antarctic Bottom Water. Thus, the relatively shallow erosion observed on the Kerguelen Plateau has almost certainly resulted from high current velocities associated with eastward flow of the Antarctic Circumpolar Current.

In the South Indian Basin, major eastward current flow occurs in the northern sector (Fig. 1). Because of the considerable depth of the basin, this flow must be related to movement of Antarctic Bottom Water, which in this area originates almost entirely from the Ross Sea. The Antarctic Bottom Water initially flows westward close to the Antarctic continent as part of the East Wind Drift (*11, 12*). We infer a relatively weak westerly flow along the up-

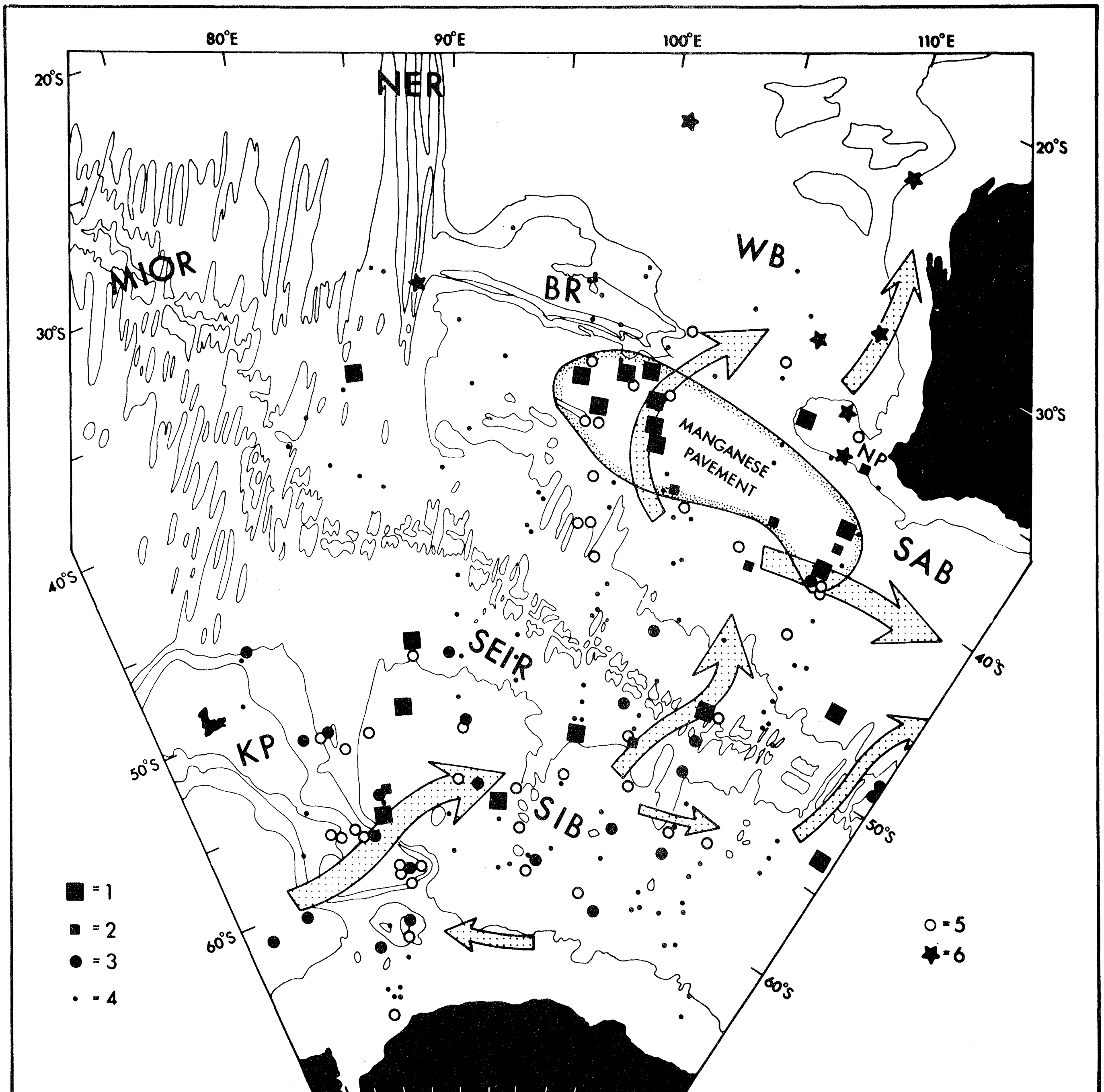

Fig. 1. Map showing sea floor dynamic processes inferred for the southeast Indian Ocean. Bathymetric contours for 2000, 3000, and 4000 m are from Heezen *et al.* (*13*). Major physiographic features are *NER*, Ninetyeast Ridge; *MIOR*, Mid-Indian Ocean Ridge; *BR*, Broken Ridge; *WB*, Wharton Basin; *NP*, Naturaliste Plateau; *SAB*, South Australian Basin; *SEIR*, Southeast Indian Ridge; *KP*, Kerguelen Plateau; and *SIB*, South Indian Basin. Symbols marking sites of interpreted observations based on bottom photographs or sediment core analyses are explained as follows: 1, manganese nodule pavement to abundant manganese nodules; 2, common to scattered manganese nodules; 3, strong bottom current activity (including ripple marks, scour, and distinct lineations); 4, core or photograph showing minimal evidence of current activity; 5, *Eltanin* piston cores featuring disconformities (*6*); and 6, site of Deep-Sea Drilling Project core featuring major disconformity (*16, 17*). The foot-shaped area shows the inferred limits of the Southeast Indian Ocean Manganese Pavement. Large arrows denote inferred paths and directions of major bottom water flow in the region. For detailed data see (*6*), and for discussion see text.

per continental rise of Antarctica, similar to that in areas to the east (*2, 5, 11*). When it comes into contact with the north-south trending Kerguelen Plateau, the Antarctic Bottom Water will be diverted first to the north and then to the east (*13*), where our evidence indicates strong erosive activity in northern parts of the South Indian Basin.

The South Indian Basin is separated from the South Australian Basin to the north by the Southeast Indian Ridge (Fig. 1). A major problem in mapping deep bottom water circulation in the Southeast Indian Ocean is locating the supply route for bottom waters northward to the western sector of the South Australian and Wharton Basins, where the geologic evidence shows major erosive activity by deep bottom waters. The two major basins in the northern part of the Indian Ocean, the Bengal and Wharton Basins, are divided by the continuous north-south trending Ninetyeast Ridge and hence must receive separate branches of Antarctic Bottom Water from the south. The temperature of the Bengal Basin water, which is nearly a degree warmer then the Wharton Basin water (*13*), confirms this point. There appear to be two possible supply routes to the South Australian and Wharton Basins (see Fig. 1). The first is via a broad sector of the mid-ocean ridge northeast of the Kerguelen Plateau, where water depths range from about 3000 to 5000 m. The second is northward through some sector of the east-west trending Southeast Indian Ridge. None of our data suggest any major bottom water transport northeast of the Kerguelen Plateau. On the contrary, this area has experienced relatively quiescent bottom conditions as far westward as 110°E. Evidence for strong bottom current activity does occur, however, in narrow zones on the Southeast Indian Ridge at 110°E and at 120°E, suggesting that the supply route of bottom water to the South Australian Basin may occur in this area (Fig. 1). This interpretation differs from that of Burckle *et al.* (*14*) who, on the basis of the distribution of Antarctic diatoms apparently dispersed northward by Antarctic Bottom Water, postulated a major northward flow between 95°E and 100°E. All of the bottom photographs and piston cores we have analyzed from this area, however, show no evidence of major bottom current activity. On the other hand, if the proposed conduit is very narrow, its effect may not be detectable by our methods.

In the western part of the South Australian Basin, Antarctic Bottom Water flows in two directions. A major eastward flow through the basin eventually supplied highly active bottom waters to the South Tasman Basin south and east of Tasmania (*2*). Another major current flows northward through the western sector, creating substantial erosion and the development of the Southeast Indian Ocean Manganese Pavement. This northward flow continues to the Wharton Basin through a gap between the east-west trending Broken Ridge and Naturaliste Plateau (Fig. 1), which themselves form major barriers to any northward deep flow. Within this basin and on the continental margin of Western Australia, the presence of highly condensed Cenozoic sequences or major Cenozoic disconformities (*15, 16*) indicates that northward-flowing erosive bottom waters have been a major long-term feature of the southeast Indian Ocean.

In conclusion, we have demonstrated that sediment of the deeper parts of the southeast Indian Ocean and the Kerguelen Plateau have been subjected to long-term erosion or diminished accumulation rates. In the former regions this dynamic activity has been intimately associated with development of a major manganese nodule field.

J. P. KENNETT
N. D. WATKINS
Graduate School of Oceanography, University of Rhode Island, Kingston 02881

References and Notes

1. N. D. Watkins and J. P. Kennett, *Science* **173**, 813 (1971).
2. ——, *Anarct. Res. Ser. (Am. Geophys. Union)* **19**, 273 (1972).
3. D. A. Johnson, *Geol. Soc. Am. Bull.* **83**, 3121 (1972).
4. H. G. Goodell, *Am. Geogr. Soc. Antarct. Map Folio Ser. Folio 17* (1973), p. 1.
5. C. D. Hollister and B. C. Heezen, *Johns Hopkins Oceanogr. Stud.* **3**, 177 (1967).
6. J. P. Kennett and N. D. Watkins, *Geol. Soc. Am. Bull.*, in press.
7. H. G. Goodell and N. D. Watkins, *Deep-Sea Res.* **15**, 89 (1968).
8. B. C. Heezen and C. D. Hollister, *The Face of the Deep* (Oxford Univ. Press, New York, 1971).
9. J. R. Connolly and R. R. Payne, *Antarct. Res. Ser. (Am. Geophys. Union)* **19**, 295 (1972).
10. R. E. Houtz, personal communication.
11. A. L. Gordon, *Antarct. Res. Ser. (Am. Geophys. Union)* **15**, 169 (1971).
12. P. Rodman and A. L. Gordon, personal communication.
13. B. C. Heezen, M. Tharp, C. R. Bentley, *Am. Geogr. Soc. Antarct. Map Folio Ser. Folio 16* (1972).
14. L. H. Burckle, W. H. Abbot, J. Maloney, *EOS (Trans. Am. Geophys. Union)* **54**, 336 (1973).
15. T. A. Davies, O. E. Weser, B. P. Luyendyk, R. B. Kidd, *Nature (Lond.)* **253**, 15 (1975).
16. J. J. Veevers, J. R. Heirtzler, *et al.*, *Initial Reports of the Deep-Sea Drilling Project* (Government Printing Office, Washington, D.C., 1974), vol. 27.
17. T. A. Davies, B. P. Luyendyk, *et al.*, *Initial Reports of the Deep-Sea Drilling Project* (Government Printing Office, Washington, D.C., 1974), vol. 26.
18. Supported by the National Science Foundation, Office of Polar Programs, grant OPP 71-04027 to J.P.K. and grants OPP 74-18529 and GV 25400 to N.D.W. We appreciate the technical assistance of A. Doherty and N. Healy.

3 March 1975

Vitamin D: 3-Deoxy-1α-Hydroxyvitamin D_3, Biologically Active Analog of 1α,25-Dihydroxyvitamin D_3

Abstract. *The ability of chemically synthesized 3-deoxy-1α-hydroxyvitamin D_3, an analog of the biologically active form of vitamin D_3 (1α,25-dihydroxyvitamin D_3), to stimulate intestinal calcium transport was assessed. The 3-deoxy analog acted significantly more rapidly than vitamin D_3 and only slightly slower than 1α,25-dihydroxyvitamin D_3. Comparison of the dose-response curves of these three vitamin D derivatives emphasizes the importance of the 3β-hydroxyl group to biological activity.*

For vitamin D to carry out its classical biological functions in stimulating intestinal calcium transport and mobilizing bone calcium, it must first be hydroxylated on C-25 (*1*) in the liver and then on C-1 by the kidney (*2*). The metabolite produced, 1α,25-dihydroxyvitamin D_3 [1α,25-$(OH)_2$-D_3], is considered to be the hormonally active form of vitamin D_3 (*3*); it is the most rapid and highly biologically active form of the vitamin in terms of stimulating intestinal calcium transport (*4*) or bone calcium mobilization (*5*). The mode of action of 1α,25-$(OH)_2$-D_3 in the intestine is believed to be analogous to that of other steroid hormones: it first associates with a cytoplasmic receptor (*6*), then is transferred to the nucleus where it associates with the chromatin (*7*), which results ultimately in synthesis of calcium-binding protein (*8*) and enhancement of calcium transport.

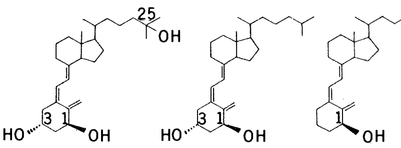

1 **2** **3**

Fig. 1. Structures of 1α,25-$(OH)_2$-D_3 (**1**), 1α-OH-D_3 (**2**), and 3-D-1α-OH-D_3 (**3**).

Because of the number of pathological conditions that might be due to abnormalities in vitamin D metabolism, it is of interest to determine the relationships between the chemical structure of 1α,25-$(OH)_2$-D_3 and its biological function in the target organ. The osteomalacia and hypocalcemia associated with uremia, vitamin D–resistant rickets, or antagonism of vitamin D action by anticonvulsant drugs have all been related in some degree to abnormalities in vitamin D metabolism (*9*). Norman, Coburn, and co-workers (*10*)